RESEARCH ARTICLE Indian Journal of Animal Research, Volume 60 Issue 2: 210-217 (February 2026)

Impact of *Theileria annulata* on Hemato-biochemical and Histological Parameters in Cattle

Haleema Y. Alnahari[1], Taghreed H. Alwuthaynani[1], Haleema H. Albohiri[1], Muslimah N. Alsulami[1] 10.18805/IJAR.BF-1933

ABSTRACT

Background: *Theileria* Spp. is the causative agent of the economically significant hemoprotozoan disease known as theileriosis in cattle. In dairy animals, it results in death and decreased productivity. This study aimed to clarify the effects of *Theileria annulata* (*T. annulata*) infection on the histological and haemato-biochemical parameters in infected cattle.

Methods: Between December 2022 and May 2023, 200 cattle were randomly selected from the slaughterhouse and blood samples were collected from them to assess the hemato-biochemical parameters and screen for *T. annulata* infection using a Giemsa-stained blood smear, furthermore, the histological profile of the spleen, lymph nodes and liver.

Result: *T. annulata* was detected in 26.5% of the cattle based on blood smear microscopy. The haematological analysis showed a notable increase in lymphocytes and a significant drop in platelets, haemoglobin, total leukocyte count and total erythrocyte count. In cattle infected with *T. annulata*, biochemical examination showed a significant increase in alanine aminotransferase (ALT), aspartate aminotransferase (AST), high density lipoprotein (HDL) and triglyceride, also increase in bilirubin. Histological examination revealed necrotic degenerations of splenic nodules, oedema, parenchymal necrotic degeneration, increased intercellular spaces, depletion of lymphocytes, increased sinuses in lymph nodes and focal necrosis of hepatocytes with infiltration of inflammatory cells and vacuolar degeneration of hepatocytes.

Key words: Blood smear, Cattle, Hemato-biochemical, Pathological alternations, Theileriosis.

INTRODUCTION

Bovine Tropical Theileriosis is a tick-borne disease (TBD). Commonly known as “Theileriosis.” globally distributed and caused by the hemoprotozoan parasite *T. annulata*. According to (El Damaty *et al.,* 2022), tropical bovine theileriosis poses a significant risk to around 250 million cattle globally, hence adversely affecting animal productivity, particularly in developing countries. Accordingly, this disease limits the development programs of several breeds, reduces production and induces higher farm mortality rates (Ullah *et al.,* 2021). According to (Mohammed *et al.,* 2018), ticks belonging to the genus Hyalomma are responsible for transmitting *T. annulata*, but Ixodid ticks can spread *Thielaria* cross-stadially. *T. annulata* sporozoites observed in tick saliva transmit the infection from ticks to their bovine host. The sporozoites enter the lymph nodes after invading the host’s circulation. Here, they reproduce asexually to infect and transform the lymphocytes into the schizont stage (Al-Hosary *et al.,* 2024). After maturing into piroplasms that infect erythrocytes, feeding ticks may later acquire the schizonts (Liu *et al.,* 2022).

Clinical symptoms suggestive of theileriosis, like swollen anorexia, pyrexia, loss of condition, pale mucous membranes and lymph nodes are used to make a tentative diagnosis. Microscopic analysis of Giemsa-stained blood smears, serological and molecular tests and lymph node fine needle aspirate smears assure the diagnosis (Agina *et al.,* 2020). When the disease is acute, thin smears of blood and lymph nodes stained with Giemsa and Wright are usually used to diagnose theileriosis (Riaz *et al.,* 2023).

[1]Department of Biological Sciences, College of Science, University of Jeddah, Jeddah, Saudi Arabia.

Corresponding Author: Muslimah N. Alsulami, Department of Biological Sciences, College of Science, University of Jeddah, Jeddah, Saudi Arabia. Email: mnal-sulami@uj.edu.sa

How to cite this article: Alnahari, H.Y., Alwuthaynani, T.H., Albohiri, H.H. and Alsulami, M.N. (2026). Impact of *Theileria annulata* on Hemato-biochemical and Histological Parameters in Cattle. *Indian Journal of Animal Research*. **60(2):** 210-217. doi: 10.18805/IJAR.BF-1933.

Submitted: 03-12-2024 **Accepted:** 02-05-2025 **Online:** 19-03-2025

Blood and biochemical profiles, such as bilirubin, cholesterol, albumin, glucose, urea, creatinine, also total proteins, can be useful within diagnosing several diseases. Serum levels of AST and ALT enzymes provide a base directory of the state of the liver and muscles. In veterinary studies, these hemato-biochemical data efficiently discriminate between healthy and diseased animals (Riaz and Tasawar, 2017). One of the most important criteria necessary to determine the health status of the animal is the Haematological parameters. These include total erythrocyte count, hematocrit, haemoglobin concentration, mean corpuscular volume, also mean corpuscular haemoglobin concentration, total and differential leukocyte count (Al-Hamidhi *et al.,* 2021).

Plasma biochemistry can be a useful diagnostic and treatment evaluation tool and a potential indicator of the infection’s severity. Additionally, based on the factors above, some biochemical criteria may be established to precisely

characterize the disease and comprehend the host-parasite relationship at a molecular level (Abubakar *et al.,* 2019).

The study aimed to determine the prevalence of theileriosis in cattle and examine its impact on hemato-biochemical and histological parameters in cattle carrying *T. annulata.*

MATERIALS AND METHODS

Study Design and Sample Collection

In the central slaughterhouse, 200 total of cattle were slaughtered in Jeddah city in the west of Saudi Arabia (Fig 1) from December 2022 to May 2023. Five milliliters of blood were aseptically collected from the jugular vein, 2.5 mL was taken without anticoagulants to separate serum for biochemical analysis and 2.5 mL was taken with EDTA for complete blood count (CBC). Samples were processed after storage at low temperature during transportation to the laboratory and sera to be tested were collected in Eppendorf and stored at -20°C until used for biochemical analysis.

Blood smear microscopic examination

The blood samples were examined for intra-erythrocytic piroplasms of *T. annulata* using microscopy. Blood samples were prepared into thin smears, air-dried, fixed in 96% methanol for five minutes and stained with 5% Giemsa stain for thirty minutes. Each slide was examined under a compound microscope with a 100x objective lens. A single observer independently examined over thirty microscopic fields in each smear, determining a slide's positivity even if a single piroplasm organism was present (Kumar *et al.,* 2022).

Assessment of haematological parameters

The study assessed haematological parameters in healthy and infected cattle using a haematology analyzer, determining total erythrocyte, leukocyte, haemoglobin, platelets, hematocrit and lymphocyte counts (Mahmoud *et al.,* 2019).

Assessment of biochemical parameters

Via spectrophotometric analysis in a clinical chemistry analyzer, the serum biochemical parameters were determined following the manufacturer's instructions utilizing commercially available kits. The levels of various biomarkers were compared in infected and healthy animals, including total protein, albumins, globulins, A/G ratio, aspartate amino transferase (AST), alanine aminotransferase (ALT), gamma-glutamyl transferase (GGT), cholesterol, High density lipoproteins (HDL), low-density lipoproteins (LDL), triglycerides and total bilirubin.

Assessment of histological examination

The spleen, lymph nodes and liver tissues were fixed in 10% formalin, dehydrated with alcohol, cleaned in xylene, embedded and blocked in paraffin. Hematoxylin and eosin (H and E)-stained sections measuring 5 µm in thickness were placed on glass slides and examined under a light microscope to examine the minute alterations in both infected and uninfected tissues (Li *et al.,* 2018).

Statistical analysis

The data was analyzed using SPSS software (SPSS for Windows Version 22, SPSS Inc., Chicago, USA) withcategory variables examined using the Chi-square test and the student's t-test. A statistically significant difference was defined as $P<0.05$ and $P<0.01$, indicating a difference between two groups.

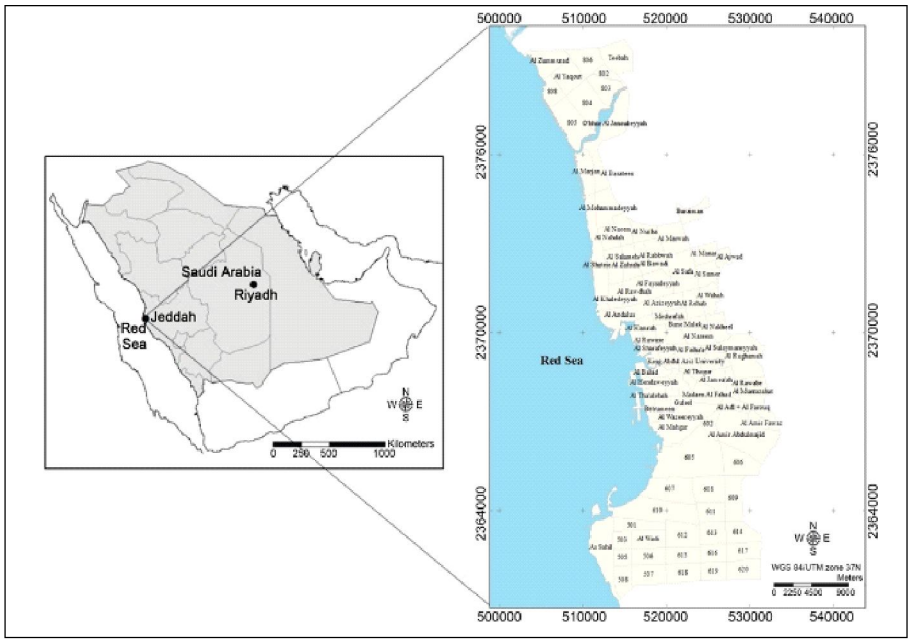


Fig 1: Map of the study area in Jeddah city in Saudi Arabia (Hamza *et al.,* 2016).

RESULTS AND DISCUSSION

Prevalence of *T. annulata* infection in cattles

The detection of *T. annulata* was found in 26.5% of the samples, out of a total of 53/200. The diagnosis of *T. annulata* was confirmed by examining various intraerythrocytic forms on Giemsa-stained blood smears, primarily signet rings but also comma and dot-shaped forms. Our results concur with (Nayel *et al.,* 2012), who found *T. annulata* in 20.89% of cattle in the Delta region of Egypt. El Damaty *et al.* (2022) found that 70% of cattle were infected with *T. annulata* through an indirect antibody fluorescence test. Microscopical examination is commonly used in veterinary clinical settings to identify acute theileriosis in disease-endemic regions, despite its low sensitivity and specificity due to unavailability of diagnostics.

Hematological findings

The haematological profiles show a highly significant decrease in (RBC), (WBC) and haemoglobin in cattle infected with *T. annulata*. In contrast, the lymphocyte counts significantly increased (P<0.01). The platelet count decreased significantly (P<0.05), but the hematocrit percentage showed no significant difference (P>0.05) (Table 1).

The study's findings align with previous research by (Agina *et al.,* 2021; Abdullah *et al.,* 2022; Farooq *et al*., 2019; Krishnamoorthy *et al.,* 2021; Ahmad *et al.,* 2023). This may result from higher oxidative stress in infected animals, which causes erythrocyte fragility from membrane breakage and a decrease in haemoglobin content. The spleen lymph nodes and other organs' endothelial systems may have phagocytosed the infected cells, explaining the reduction in erythrocyte count, might be due to removal of the parasitized erythrocytes by reticuloendothelial system.

Infected animals had a significant decrease in total leukocytes. This result is consistent with that of (Kachhawa *et al.,* 2016), who observed a significant decline in white blood cells. Decreases hematopoietic activity combined with systemic devastation of piroplasm-infected RBCs by macrophages in lymph nodes, spleen and other immune system organs may result in leukopenia (Narang *et al.,* 2019). According to (Ahmadi *et al.,* 2020), the study revealed a significant increase in the lymphocyte count., which could be attributed to two compensatory mechanisms acting as target cells in response to *Theileria* invasion. Additionally, we found that the platelet counts of the infected cattle had significantly decreased. This outcome is consistent with (Shah *et al.,* 2020). This may result from immune-mediated destruction, sequestration of platelets in the spleen and systemic and local disseminated intravascular coagulation.

Biochemical findings

Infected cattle had a highly significant increase in ALT, AST, HDL and triglyceride in their serum biochemical profile. However, infected cattle significantly decreased LDL, albumin, total protein, cholesterol and GGT.

Table 1: Comparison of haematological parameters in the infected and non-infected cattle.

Parameters/units	Non-infected (N=147)	Infected (N=53)	*P-value*
Red blood cell (10^6/µl)	6.68±0.33	5.48±0.30	0.01^{HS}
White blood cell (10^3/µl)	9.09±0.20	8.17±0.19	0.002^{HS}
Hemoglobin (g/d)	11.28±0.60	7.38±0.59	0.003^{HS}
Hematocrit (%)	30.63±0.13	30.97±0.16	0.09^{NS}
Platelets (10^3/µl)	727.55±18.69	673.63±18.72	0.04^{S}
Lymphocytes (%)	27.54±1.94	36.04±1.33	0.002^{HS}

NS: Non-significant at p-value ≥0.05; S: Significant at p-value <0.05; HS: Highly significant at p-value < 0.01.

Table 2: Effect of *T. annulata* infection on biochemical parameters in cattle.

Parameters/unit	Non-infected (N=147)	Infected (N=53)	*P-value*
Alanine aminotransferase (U/l)	99.1±2.95	126.75±6.61	0.01^{HS}
Aspartate aminotransferase (U/l)	85.01±3.00	91.88±0.83	0.04^{S}
Gamma-glutamyl transferase (U/l)	54±2.63	33.21±2.59	0.0007^{HS}
Total protein (g/dl)	9.06±0.26	7.31±0.55	0.04^{S}
Albumin (g/dl)	4.73±0.29	3.06±0.23	0.0002^{HS}
Globulin (g/dl)	4.33±0.13	4.26±0.35	0.81^{NS}
Albumin / Globulin ratio	1.36±0.07	5.03±0.49	0.0001^{HS}
Cholesterol (mg/dl)	254.13±11.55	211.63±21.13	0.04^{S}
High-density lipoprotein (g/dl)	29±2.43	42.38±3.81	0.006^{HS}
Low-density lipoprotein (g/dl)	225.13±12.74	170.38±9.78	0.004^{HS}
Triglyceride (g/dl)	113.63±1.26	122.75±3.09	0.01^{HS}
Total bilirubin (g/dl)	1.40±0.11	1.62±0.10	0.16^{NS}

NS: Non-significant at p-value ≥0.05; S: Significant at p-value <0.05; HS: Highly significant at p-value < 0.01.

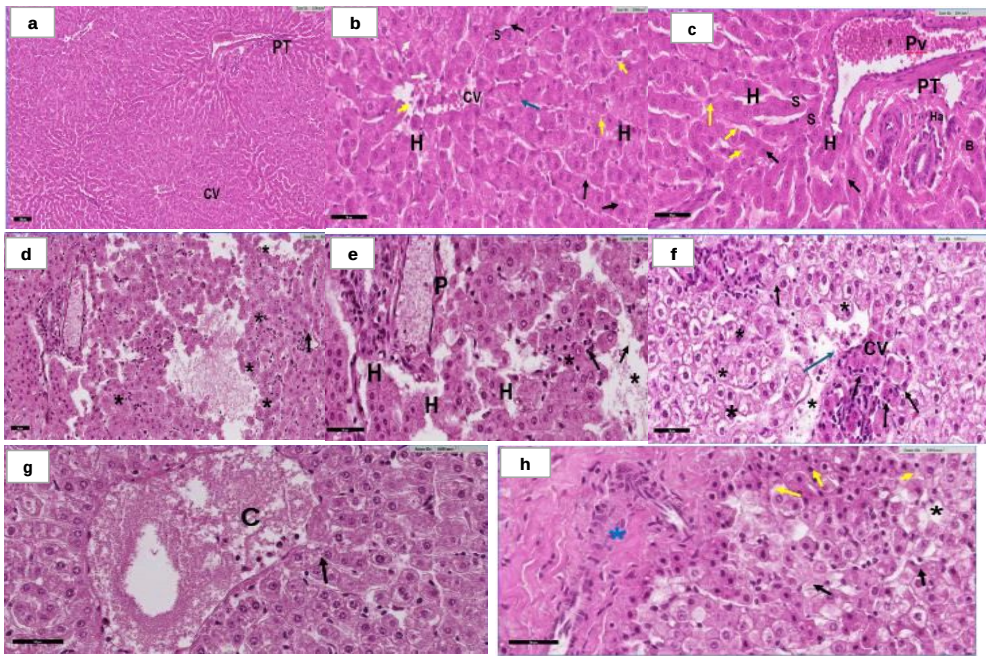
Additionally, a slight difference was observed between globulin and total bilirubin (Table 2). Infected animals had significantly higher levels of bilirubin, ALT and AST. These findings are consistent with (Beck *et al.,* 2019) and (Ahmadi *et al.,* 2020). This outcome could be the result of enhanced RBC lysis or hepatocyte necrosis and degeneration.

The total protein, albumin and globulin levels of infected cattle showed a significant decrease in our study. (Agina *et al.,* 2021) are contradicted by these results. Inflammatory disease, the deleterious effects of Theileria's toxic metabolites, or albumin loss through urine could all be responsible for this. According to our findings, triglycerides and HDL levels in infected cattle were significantly elevated. This result concurs with (Ahmadi *et al.,* 2020). A portion of this can be attributed to the liver's compensatory response to protein loss, particularly HDL.

Histological studies results

Liver

The liver of healthy control cattle was examined using H and E-stained sections, which revealed a well-definedclassic hepatic lobule with typical hepatic architecture. The typical lobule consisted of hepatocyte cords that extended from the central vein to the periphery of the lobule. The central vein, with thin walls, is lined by flat endothelial cells. The hepatocytes had a polyhedral morphology, featuring vesicular nuclei that were lightly stained, finely granular basophilic patches and acidophilic vacuolated cytoplasm. Hepatic blood sinusoids were found to be located between

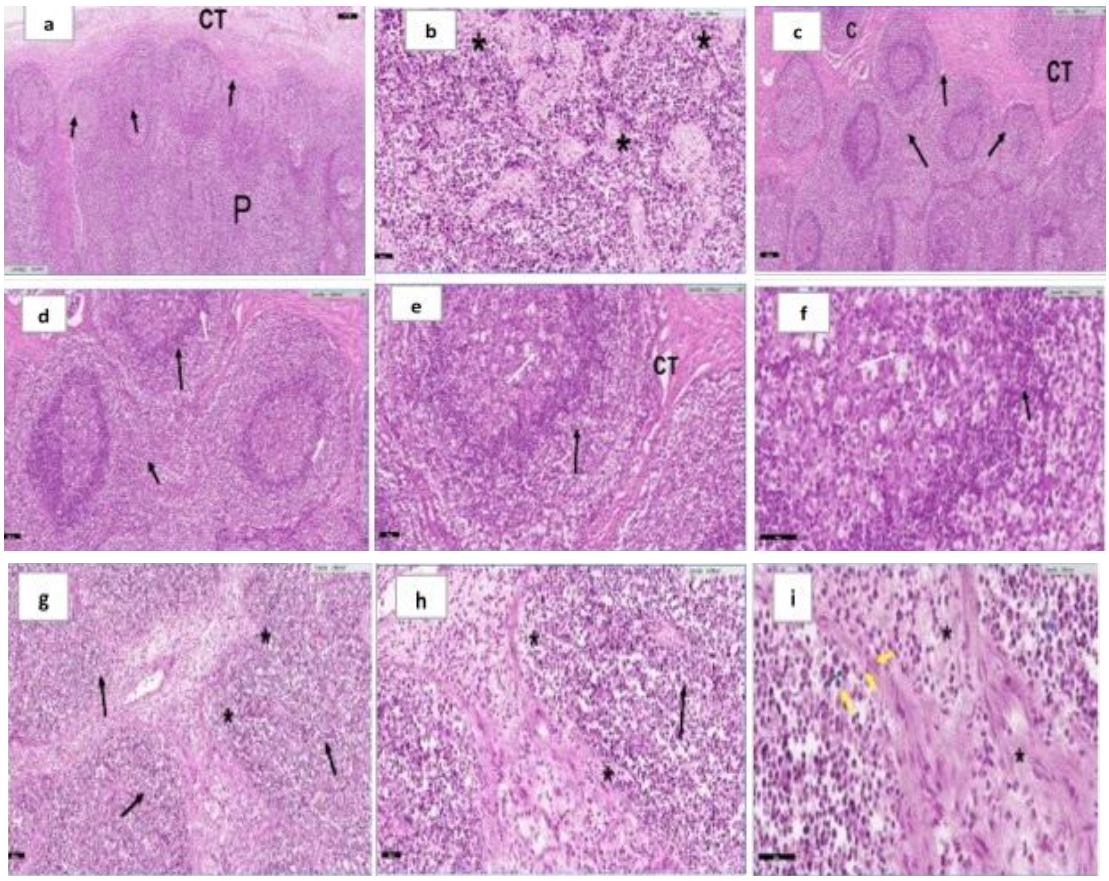


a: Normal appearance of hepatic parenchyma. The liver lobules' boundaries are unclear but can be identified by the presence of central veins (CV) and peripheral portal tract (PT) (H and E X100), **b**: The thin-walled central vein (CV) lined with flat endothelial cells (blue arrows) , eosinophilic cytoplasm with basophilic granules and the normal hepatocytes (H) with rounded vesicular nuclei (yellow arrows), while the blood sinusoids (S) between hepatocyte cell cords are lined with endothelial cells (black arrows) and von Kupffer cells (white arrows) (HandE X400), **c**: The portal tract (PT) contained a branch of the hepatic artery (Ha), a bile duct (Bd) branch of the portal vein (Pv). The blood sinusoids (S) between the hepatocyte cell cords (H) are lined with endothelial cells (white arrows) and Kupffer cells (black arrows). The hepatocytes with eosinophilic cytoplasm (H) and rounded vesicular nuclei (yellow arrows) were observed (H and E X400). The liver section from cattle infected with *T. annulata* and stained by Hematoxylin and Eosin, **d**: Necrotic degenerations of hepatocytes leaving empty spaces (*) and leukocytic infiltration (black arrows) (H and E X200), **e**: Necrotic degenerations of hepatocytes leaving empty spaces (*) and leukocytic infiltrations (black arrows) (HandE X400). Small hepatocytes (H) with deeply stained necrotic nuclei were observed around the portal tract (PT), **f**: Vacuolar degeneration of hepatocytes and vocal area of necrosis (*); degeneration in the endothelial cells (blue arrow) lining the central vein (CV) and leukocytic infiltrations (black arrow) (H and E X400), **g**: Dilatation and congestion in the central vein (blue arrow) with leukocytic infiltrations (black arrow) (H and E X400), **h**: Vacuolar degeneration of hepatocytes (*); Some cells appeared small with deeply stained pyknotic nuclei (yellow arrows) and fibrosis between the hepatocytes (blue star) with leukocytic infiltrations (black arrows) (H and E X400).

Fig 2: Photomicrograph of control cattle liver stained with H and E stain.

the hepatic cell cords, which are covered with endothelium and Kupffer cells. The bile duct, hepatic artery and portal vein branches are situated at the periphery of the portal tracts in the lobules (Fig 2a, 2b and 2c).

In cattle with *T. annulata* infection, the liver parenchyma became disorganized, the hepatic tissue plates lost their typical radial structure around the central vein and there were lymphocytic infiltrations and necrotic degenerations of hepatocytes that left empty spaces (Fig 2d and 2e). Specific hepatocytes in the specimens had strongly stained pyknotic nuclei and severely vacuolated cytoplasm (vacuolar degenerations). Along with hepatocyte vacuolar degeneration and a necrotic vocal area, there was also a noticeable lymphocytic infiltration in the portal area. Certain specimens showed leukocytic infiltrations and degeneration of the endothelial cells lining the central vein (Fig 2f). Certain specimens showed dilatation, congestion in the central vein and leukocytic infiltrations (Fig 2g). *T. annulata* caused the liver's histological abnormalities. HandE-stained sections revealed portal and central vein dilation and congestion (Fig 2e and 2g). There was significant fibrosis between the hepatocytes and several



a: Normal appearance of cortex with aggregation of secondary lymph nodule (black arrows) and paracortex (P). The connective tissue capsule surrounds the lymph node (CT) (H and E X50), **b**: a normal appearance of the medulla in the form of medullary cords (*). The cords are composed of plasma cells, B-cells and T-cells (HandE X200), **c**: a normal appearance of cortex with aggregation of secondary lymph nodule (black arrows) separated by connective tissue septa (CT). (H and E X50), **d**: The secondary lymph nodule with central germinal center (white arrows) and peripheral dark zone (black arrows) (HandE X100), **e**: A magnified part of the previous section showing the secondary lymph nodule with central germinal center (white arrow) and peripheral dark zone (black arrow). The connective tissue septa (CT) between the lymph nodule (H and E X200), **f**: A magnified part of the previous section showing the secondary lymph nodule with central pale germinal center (white arrow) and peripheral dark zone (black arrow) (H and E X400). The lymph node section from cattle infected with *T. annulata* and stained by H and E stain, **G**: Necrotic degenerations of lymph nodule (black arrows); edema and leukocytic infiltrations in the connective tissue septa (*) (H and E - X100), **h**: Necrotic degenerations of lymphocytes in the lymph nodule (black arrows); edema and leukocytic infiltrations in the connective tissue septa (*) (H and E - X200), **i**: A magnified part of the previous section from cattle infected with *T. annulata* showing edema and leukocytic infiltrations in the connective tissue septa (*). The presence of plasma cells (yellow arrows) and macrophages (blue arrows) in-between the lymphocytes (H and E - X400).

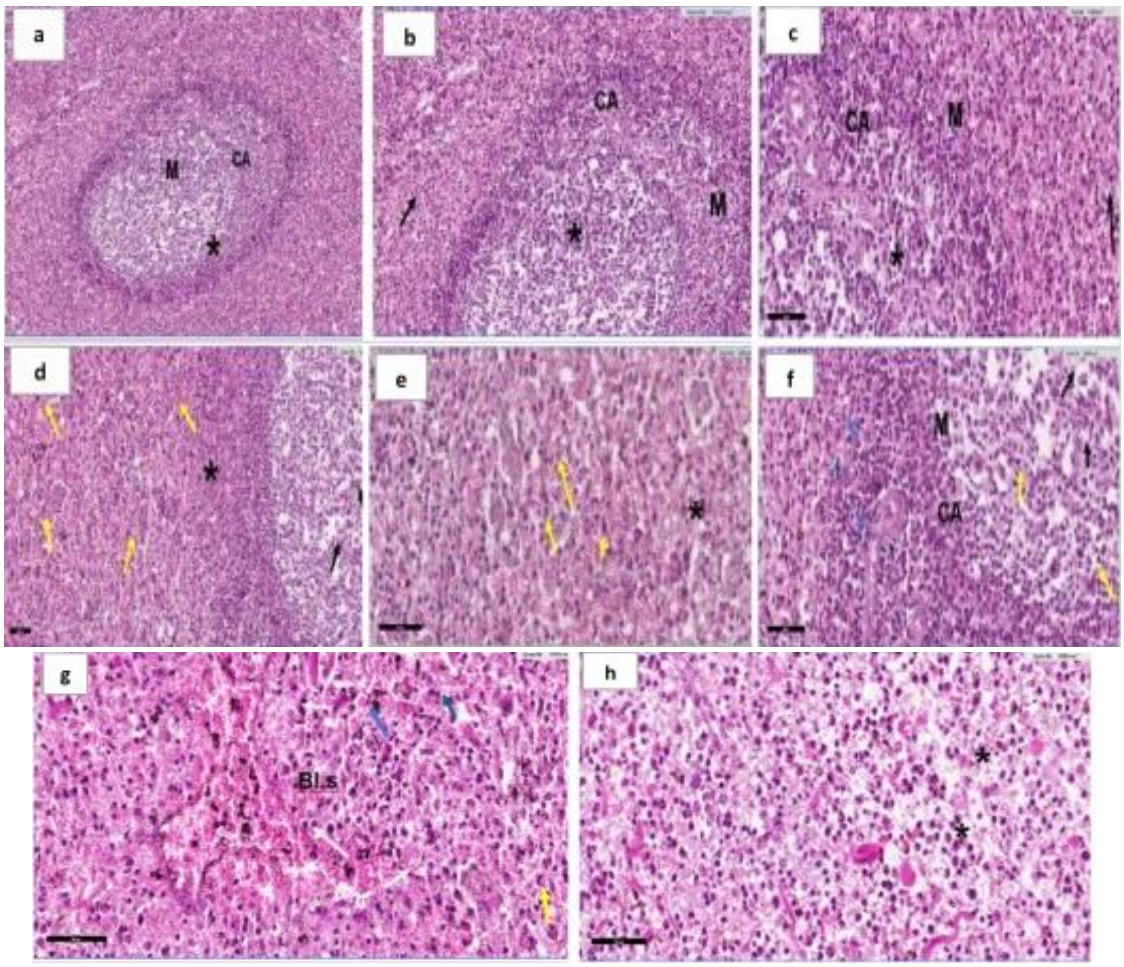
Fig 3: Photomicrograph of control cattle lymph node stained with H and E stain.

of the hepatocytes had small appearances, strongly stained pyknotic nuclei and lymphocyte infiltration (Fig 2h).

These outcomes concur with the findings of (Omer *et al.,* 2021). A significant degree of fibrosis was observedbetween the hepatocytes and specific cells had small, deeply stained pyknotic nuclei along with lymphocyte, plasma cell, macrophage and eosinophil infiltration. The significant liver damage observed during the necropsies caused the increase in AST activity.

Lymph node

A lymph node's histological sections show that it is divided into three regions: the medulla, paracortex and outer cortex and that it is surrounded by a connective tissue capsule (Fig 3a and 3b). The paracortex lies deep within the cortical layer. Its edges merge with the deep medulla and superficial cortex. The two main characteristics that set them apart are the high concentration of T lymphocytes in the paracortex'sstroma and the absence of lymphoid



a: The control spleen is depicted with white pulp (*), central artery (CA) and red pulp (black arrows). The marginal zone (M) is a boundary that separates white pulp from red pulp (H and E X100), **b**: The control spleen is depicted with white pulp (*), central artery (CA) and red pulp, with black arrows. The marginal zone (M) separates the red pulp from the white pulp (HandE X200), **c**: Control spleen shows the red pulp (black arrows) and the white pulp (white arrows) with the central artery (CA). The marginal zone (M) separates the red pulp from the white pulp (H and E X400). The spleen section from cattle infected with *T. annulata* stained with H and E stain; **d**: Necrotic degenerations of white pulp (black arrows) leaving empty spaces; and appearance of the schizont of *Theileria* (yellow arrow) in the red pulp (*) (H and E X200), **e**: The appearance of the schizont of *Theileria* (yellow arrows) in the red pulp(*) (H and E X400), **f**: Necrotic degenerations of white pulp (black arrows) leaving empty spaces; and appearance of the schizont of *Theileria* (yellow arrow) in the white pulp. The presence of pigments (hemosiderin deposition) in the red pulp (blue arrows); the marginal zone(M) and the central artery (CA) (H and E X400), **g**: The dilated blood sinusoid(bl.s) in the red pulp contains hemosiderin pigments (white arrows). Also, note the appearance of the schizont of Theileria (yellow arrow) and the presence of pigments (hemosiderin deposition) in the red pulp (blue arrows) (H and E X400), **h**: The red pulp is experiencing degeneration and depletion of cells, leaving empty spaces (*) (H and E X400).

Fig 4: The photomicrograph shows a spleen of a cattle, stained with HandE stain.

nodules (Fig 3a). The medulla is the lymph nodes deepest layer. The medullary cords and sinuses are the two additional regions into which it is separated functionally and histologically.

Along with B and T cells, plasma cells also occupy the cords. The cells are organized into centrally extended cord-like projections from the paracortex (Fig 3b). The cortex is the outermost layer. Lymphoid nodules, a cortical sinus and a subcapsular sinus comprise it. Whether a primary or secondary follicle is separated from the other by connective tissue septa determines whether or not these lymphoid nodules have a germinal center. Cattle lymph nodes are diverse collections of large B lymphocytes, primarily formed by secondary follicles, which have been stimulated by antigens (Fig 3c, 3d, 3e and 3f).

The lymph nodes of infected animals showed larger intercellular spaces, depletion of lymphocytes, oedema, parenchymal necrotic degeneration and enlarged sinuses compared to normal. Degenerative lesions, scattered necrosis of lymphocytes, haemorrhage oedema and necrosis of lymph node trabeculae are signs of hyperemia. The lymph sinus contains a variety of cells, including neutrophils, macrophages and red blood cells (Fig 3g and 3h).

(Fig 3i) show leukocytic infiltrations in the connective tissue septa and the degeneration and atrophy of lymphoid follicles. The findings are consistent with those of (Akhter *et al.,* 2017), who noted lymphocyte depletion and oedema in sheep lymph nodes.

Spleen

According to the findings of a histological examination, the parenchyma of a normal cattle spleen is composed of red and white splenic pulp separated by trabeculae and contained in a fibrous capsule. The splenic pulp is composed of two colors: red and white. The red pulp comprises sinusoids, which are amorphously scattered and meander through the pulp cord-like cellular tissue. The splenic pulp's white pulp, composed of lymphatic tissue dispersed at random, has the form of spherical-shaped lymphatic nodules with or without germinal centers and periarterial lymphatic sheaths (PALS). The central artery is located in the cross-section of PALS (Fig 4a, 4b and 4c). The splenic nodules of infected animals had necrotic degenerations of white pulp, leaving empty spaces and the appearance of the *T. annulata* schizont in the red and white pulps, according to the histopathology of the spleen (Fig 4d, 4e and 4f). White pulp deteriorated in the absence of lymphoproliferation. There was significant lymphocytic necrosis and congestion in certain splenic regions. Hemosiderin pigments were observed to be present in the red pulp (Fig 4f and 4g). Hemosiderin pigments were present in the dilated, clogged blood sinusoid in the red pulp (Fig 4 g). Additionally, it was seen that the red pulp was depleting cells and degenerating, leaving empty spaces (Fig 4h). The current results align with the findings of (Akhter *et al.,* 2017).

CONCLUSION

Numerous changes in the haematological, biochemical and histological profiles of the infected cattle with theileriosis show how this disease may damage different animal body systems, causing metabolic disruptions and severity of the disease. Haematological, biochemical and histological profiles should be taken into account for a reasonable prognosis of tropical theileriosis to facilitate early diagnosis and the timely start of a suitable treatment plan.

ACKNOWLEDGEMENT

The present study was supported by the University of Jeddah.

Disclaimers

This article's views and conclusions are solely those of the authors, not affiliated institutions. Authors are responsible for information accuracy but not liable for losses.

Informed consent

The Committee of Experimental Animal Care approved all animal procedures for experiments, while the University of Animal Care Committee approved handling techniques.

Conflict of interest

There are no conflicts of interest.

REFERENCES

Abdullah, S.H., Dyary, H.O. and Saeed, N.M. (2022). Molecular detection of *Theileria* spp. in native sheep and estimation of hemato-biochemical parameters from Sulaimani province/Iraq. *Frontiers in Veterinary Science*. **9:** 1059 599.

Abubakar, A.S., El Hussein, A.M., Abdelsalam, M.A., Salih, D.A., Samia, H.A. and Hala Elrayah, S.A. (2019). Alterations of hematological and biochemical profile of calves infected naturally with tropical Theileriosis. *American Journal of Biomedical Science and Research*. **5(3):** 218-223.

Agina, O.A., Shaari, M.R., Isa, N.M.M., Ajat, M., Zamri-Saad, M. and Hamzah, H. (2020). Clinical pathology, immunopathology and advanced vaccine technology in bovine theileriosis: A review. *Pathogens*. **9(9):** 697.

Agina, O.A., Shaari, M.R., Isa, N.M.M., Ajat, M., Zamri-Saad, M., Mazlan, M., Muhamad, A.S., Kassim, A.A., Ha, L.C., Rusli, F.H., Masaud, D. and Hamzah, H. (2021). Molecular detection of Theileria species, Anaplasma species, *Candidatus Mycoplasma haemobos*, *Trypanosoma evansi* and first evidence of Theileria sinensis-associated bovine anaemia in crossbred Kedah-Kelantan × Brahman cattle. *BMC Veterinary Research*. **17:** 1-20.

Ahmad, T., Tufani, N.A., Haq, A.U., Tramboo, S.R., Allaie, I.M., Malik, H.U., Dar, N.A. and Dar, A.A. (2023). Clinico-haemato-biochemical changes and therapeutic efficacy of diminazene aceturate and artesunate against bovine babesiosis in Kashmir valley. *Indian Journal of Animal Research*. **1:** 7. doi: 10.18805/IJAR.B-5014.

Ahmadi Afshar, N., Malekifard, F., Asri Rezaei, S. and Tavassoli, M. (2020). Hematological and biochemical changes in naturally occurring equine piroplasmosis in donkeys (*Equus asinus*) of Northwest of Iran. *Acta Parasitologica*. **65:** 811-816.

Akhter, W., Aslam, A., Rehman, M.U., Rehman, H.U., Rashid, I. and Akhtar, R. (2017). Comparative pathological changes in sheep infected with *Theileria annulata* and non-infected control. *Journal of the Hellenic Veterinary Medical Society*. **68(4):** 629-634.

Al-Hamidhi, S., Elshafie, E.I., Yaghfoori, S., Morrison, W.I., Johnson, E.H. and Babiker, H.A. (2021). A comparative study of single *Theileria lestoquardi* and mixed infections with Theileria ovis. *Parasites and Vectors*. **14:** 1-10.

Al-Hosary, A., Radwan, A.M., Ahmed, L.S., Abdelghaffar, S.K., Fischer, S., Nijhof, A.M., Clausen, P.H. and Ahmed, J.S. (2024). Isolation and propagation of an Egyptian *Theileria annulata* infected cell line and evaluation of its use as a vaccine to protect cattle against field challenge. *Scientific Reports*. **14(1):** 8565.

Beck, A., Huber, D., Antolić, M., Anzulović, Ž., Reil, I., Polkinghorne, A., Baneth, G. and Beck, R. (2019). Retrospective study of canine infectious haemolytic anaemia cases reveals the importance of molecular investigation in accurate postmortal diagnostic protocols. *Comparative Immunology, Microbiology and Infectious Diseases*. **65:** 81-87.

El Damaty, H.M., Yousef, S.G., El-Balkemy, F.A., Nekouei, O., Mahmmod, Y.S. and Elsohaby, I. (2022). Seroprevalence and risk factors of tropical theileriosis in smallholder asymptomatic large ruminants in Egypt. *Frontiers in Veterinary Science*. **9:** 1004378.

Farooq, U., Tufani, N.A., Malik, H.U. and Mir, M.S. (2019). Clinical and morpho-molecular epidemiology of bovine theileriosis in Kashmir, India. *Indian Journal of Animal Research*. **53(3):** 375-381. doi: 10.18805/ijar.B-3512.

Hamza, M.H., Al-Thubaiti, A.S., Dhieb, M., Ali, A.B.H., Garbouj, M.S. and Ajmi, M. (2016). Dasymetric mapping as a tool to assess the spatial distribution of population in Jeddah City (Kingdom of Saudi Arabia). *Current Urban Studies*. **4(3):** 329-342.

Kachhawa, J.P., Kumar, S., Sharma, A., Singh, A.P. and Ahuja, A. (2016). Studies on alterations of clinical and hemato-biochemical parameters before and after treatment in calves naturally infected with theileriosis. *Veterinary World*. **9(12):** 1381.

Krishnamoorthy, P., Akshata, L.G., Jacob, S.S., Suresh, K.P. and Roy, P. (2021). Theileriosis prevalence status in cattle and buffaloes in India established by systematic review and meta-analysis. *Indian Journal of Animal Sciences*. **91(4):** 269-279.

Kumar, A., Kumar, R., Tiwary, R., Bhoomika, Singh, G.D., Kumar, A., Gattani, A. and Shekhar, P. (2022). Clinico-morphological and molecular detection of bovine tropical theileriosis in cattle. *Indian Journal of Animal Research*. doi: 10.188 05/IJAR.B-5002.

Li, Y., Li, N., Yu, X., Huang, K., Zheng, T., Cheng, X., Zeng, S. and Liu, X. (2018). Hematoxylin and eosin staining of intact tissues *via* delipidation and ultrasound. *Scientific Reports*. **8(1):** 12259.

Liu, J., Guan, G. and Yin, H. (2022). *Theileria annulata*. *Trends in Parasitology*. **38(3):** 265-266.

Mahmoud, M.H.S., Al-Dhalimy, A.M.B. and Al-Dujaily, A.H. (2019). Study of hematological and biochemical changes in sheep and goats infected with theileriosis at Al-Najaf province. Iraq.

Mohammed-Ahmed, G.M., Hassan, S.M., El Hussein, A.M. and Salih, D.A. (2018). Molecular, serological and parasitological survey of *Theileria annulata* in North Kordofan State, Sudan. *Veterinary Parasitolog. Regional Studies and Reports*. **13:** 24-29.

Narang, A., Randhawa, S.S., Sood, N.K., Chhabra, S., Singla, L.D. and Kaur, P. (2019). Atypical theileriosis with cutaneous involvement in a cow in India: A case report. *Revue Scientifique et Technique - Office International des Epizooties*. **38(3):** 703-709.

Nayel, M., El-Dakhly, K.M., Aboulaila, M., Elsify, A., Hassan, H., Ibrahim, E., Hassan, H., Ibrahim, E., Salama, A. and Yanai, T. (2012). The use of different diagnostic tools for Babesia and *Theileria parasites* in cattle in Menofia, Egypt. *Parasitology Research*. **111:** 1019-1024.

Omer, S.A., Alsuwaid, D.F. and Mohammed, O.B. (2021). Molecular characterization of ticks and tick-borne piroplasms from cattle and camel in Hofuf, eastern Saudi Arabia. *Saudi Journal of Biological Sciences*. **28(3):** 2023-2028.

Riaz, M. and Tasawar, Z. (2017). A study on molecular diagnosis of Theileria species infection by PCR amplification in sheep and goats in Multan, Pakistan. *Biological Sciences-Pakistan Journal of Scientific and Industrial Research*. **60(1):** 36-45.

Riaz, M., Nasreen, N., Khan, A. and Said, M.B. (2023). Differential diagnosis of theileriosis through blood smear examination and polymerase chain reaction in small ruminants from Pakistan. *Open Veterinary Journal*. **13(6):** 697-704.

Shah, M.H., Ijaz, M., Ahmed, A., Aziz, M.U., Ghaffar, A., Ghauri, H.N. and Naveed, M. (2020). Molecular analysis and risk factors associated with *Theileria equi* infection in domestic donkeys and mules of Punjab, Pakistan. *Journal of Equine Veterinary Science*. **92:** 103164.

Ullah, R., Shams, S., Khan, M.A., Ayaz, S., Akbar, N.U., Din, Q.U., Khan, A., Leon, R. and Zeb, J. (2021). Epidemiology and molecular characterization of *Theileria annulata* in cattle from central Khyber Pakhtunkhwa, Pakistan. *PLOS ONE*. **16(9):** e0249417.